Role of the proto-oncogene *Pokemon* in cellular transformation and *ARF* repression

Takahiro Maeda[1,2], Robin M. Hobbs[1,2], Taha Merghoub[1,2], Ilhem Guernah[1,2], Arthur Zelent[3], Carlos Cordon-Cardo[2], Julie Teruya-Feldstein[2] & Pier Paolo Pandolfi[1,2]

[1]*Cancer Biology and Genetics Program,* [2]*Department of Pathology, Memorial Sloan-Kettering Cancer Center, Sloan-Kettering Institute, 1275 York Avenue, New York, New York 10021, USA*
[3]*Leukemia Research Fund Center at the Institute of Cancer Research, Chester Beatty Laboratories, Fulham Road, London SW3 6JB, UK*

Aberrant transcriptional repression through chromatin remodelling and histone deacetylation has been postulated to represent a driving force underlying tumorigenesis because histone deacetylase inhibitors have been found to be effective in cancer treatment. However, the molecular mechanisms by which transcriptional derepression would be linked to tumour suppression are poorly understood. Here we identify the transcriptional repressor Pokemon (encoded by the *Zbtb7* gene) as a critical factor in oncogenesis. Mouse embryonic fibroblasts lacking *Zbtb7* are completely refractory to oncogene-mediated cellular transformation. Conversely, Pokemon overexpression leads to overt oncogenic transformation both *in vitro* and *in vivo* in transgenic mice. Pokemon can specifically repress the transcription of the tumour suppressor gene *ARF* through direct binding. We find that Pokemon is aberrantly overexpressed in human cancers and that its expression levels predict biological behaviour and clinical outcome. Pokemon's critical role in cellular transformation makes it an attractive target for therapeutic intervention.

The POZ domain (for poxvirus and zinc finger; also known as the BTB domain) is a highly conserved protein–protein interaction domain found in about 250 known human proteins so far (http://www.ebi.ac.uk/interpro/IEntry?ac=IPR000210). Members of the POK (POZ and Krüppel) family of proteins contain an amino-terminal POZ domain and a carboxy-terminal DNA-binding domain made of Krüppel-type zinc fingers and can act as potent transcriptional repressors through the recruitment of histone deacetylases (HDACs) and subsequent chromatin remodelling[1,2]. POK proteins are important in embryonic development, differentiation and oncogenesis[3–7]. In particular, PLZF (for promyelocytic leukaemia zinc finger)[8] and BCL6 (for B-cell lymphoma 6)[9], two members of this POK family, are involved in chromosomal translocations associated with acute promyelocytic leukaemia and non-Hodgkin's lymphoma, respectively.

Pokemon (for POK erythroid myeloid ontogenic factor; also known as LRF[10], OCZF[11] and FBI-1 (ref. 12)) is a POK protein family member that has a critical and pleiotropic function in cellular differentiation and can physically interact with other POK family members such as BCL6 (ref. 10). *Zbtb7* inactivation in mouse results in embryonic lethality and impaired cellular differentiation in multiple tissues including the B-cell compartment (T.M. and P.P.P., unpublished data). It could therefore be proposed that perturbation of Pokemon's transcriptional function impairs cellular differentiation, as is often observed in human cancer. In a non-mutually exclusive hypothesis, Pokemon could modulate cellular functions/pathways important for oncogenic transformation, thus taking a more direct role in tumorigenesis. To test this hypothesis we therefore assessed the role of Pokemon in cancer pathogenesis through a direct genetic approach.

Role of Pokemon in oncogenesis

We initially tested whether loss of *Pokemon* function would affect the transforming potential of primary cells. To this end, we performed classic cell growth and transformation assays by taking advantage of early-passage mouse embryonic fibroblast cells (MEFs). In this experimental setting, combinations of potent oncogenes such as *E1A*+*H-ras*^{V12}, *Myc*+*H-ras*^{V12}, *T-antigen* (*T-Ag*)+*H-ras*^{V12} normally elicit a marked proliferative response in wild-type (WT) MEFs[13] (Fig. 1a). In addition, although overexpression of a single oncogene does not transform WT MEFs, combinations of oncogenes can induce cellular transformation as revealed by a colony formation assay in soft agar (Fig. 1b). Strikingly, *Zbtb7*$^{-/-}$ MEFs were completely unresponsive to both the proliferative stimulus triggered by these oncogene combinations and their transforming ability, whereas the expression levels of introduced oncogenes were comparable in WT and *Zbtb7*$^{-/-}$ MEFs (Supplementary Fig. 1a). Pokemon is therefore required for the growth-promoting and transforming activity of these combinations of oncogenes.

We next determined whether Pokemon would display proto-oncogenic activity when coexpressed in combination with other oncogenes. To this end, we infected WT MEFs with retroviruses containing *Myc*, *H-ras*^{V12}, *T-Ag* and/or *Pokemon* genes and generated a growth curve. In this experimental condition, mock-infected control cells failed to proliferate, because cells were plated sparsely and lost cell–cell contact (not shown). As described previously, MEFs infected with *Myc* alone underwent apoptosis[14], whereas expression of oncogenic *ras* resulted in premature senescence[15] (not shown). As a consequence, MEFs infected singly with *H-ras*^{V12} or *Myc* failed to proliferate (Fig. 1c). In contrast, Pokemon coexpression blocked oncogene-induced apoptosis and senescence and, as a result, MEFs co-infected with *Pokemon* and *Myc*, *H-ras*^{V12} or *T-Ag* displayed a marked proliferative advantage (Fig. 1c). Furthermore, *Pokemon*-infected Rat1 MycEr™ cells[16] were more resistant to Myc-induced apoptosis than mock-infected cells (Supplementary Fig. 1c). Strikingly, MEFs co-infected with *T-Ag*, *Myc*, *H-ras*^{V12} and *Pokemon* readily formed colonies when plated in soft agar (Fig. 1d and Supplementary Fig. 1b). Pokemon also opposed E1A-induced apoptosis[17], thus stimulating the growth of co-infected MEFs. However, *E1A* and *Pokemon* did not transform MEFs when co-infected (not shown).

Pokemon is a specific repressor of *ARF*

We set out to investigate the mechanisms by which Pokemon would exert its oncogenic activity. It has been reported that the N-terminal POZ domain of POK family members can mediate their physical interaction with a large co-repressor complex[1,2], and Pokemon is no exception to this rule (not shown). We therefore proposed that Pokemon might directly repress the expression of a pivotal tumour suppressor whose silencing would result in cellular transformation in combination with the aforementioned oncogenes. We therefore first characterized the putative Pokemon-binding sequence by CAST (for cyclic amplification and selection of targets; see Supplementary Fig. 2a, b) analysis[18] followed by electrophoretic mobility-shift assay (EMSA). Pokemon directly and specifically bound oligonucleotides containing an identified Pokemon-binding sequence *in vitro* (Supplementary Fig. 2c). Furthermore, Pokemon could repress the activity of an artificial promoter containing Pokemon-binding sites (Supplementary Fig. 2d). To identify the core binding sequence in a Pokemon-binding site, we generated a series of mutated oligonucleotides and performed EMSA assays. Two cytosine residues in the centre of consensus sequence (underlined in Fig. 2a) were revealed to be essential for Pokemon binding (Supplementary Fig. 2e–g).

Subsequently, we searched the promoters of key tumour suppressor genes for putative Pokemon-binding sites. In this respect, $p19^{Arf}$ and *p53* were legitimate candidates in view of the fact that their inactivation is known to cooperate with both *Myc* and oncogenic *ras* in neoplastic transformation[14]. We found several putative Pokemon-binding sites in the *ARF* promoter, and several

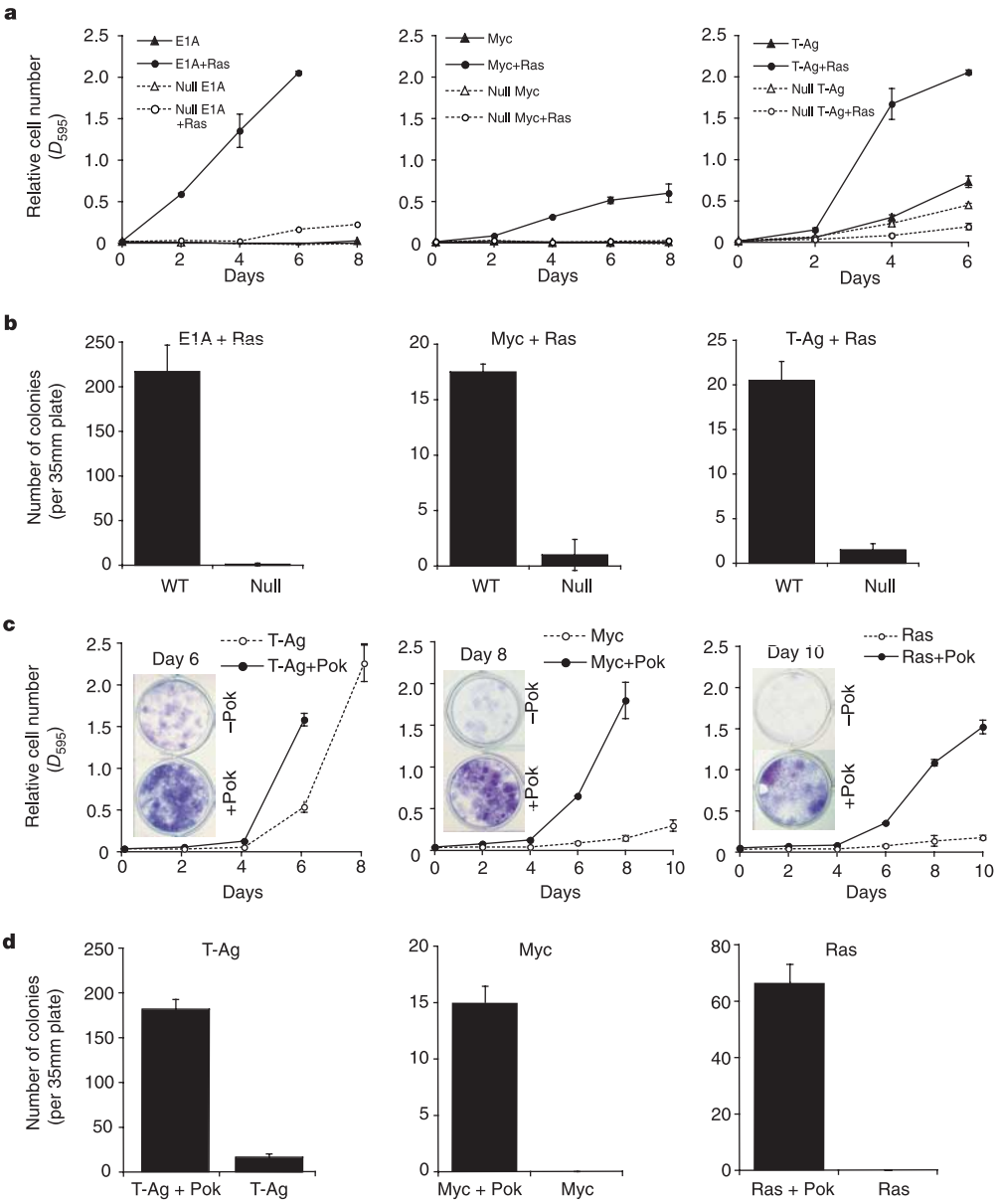

Figure 1 Pokemon is indispensable for cellular transformation and acts as a proto-oncogene. **a**, Growth curve of WT or *Zbtb7*$^{-/-}$ (Null) MEFs infected with the indicated retroviral vectors. After infection, 3,000 cells were plated per well in 12-well plates in triplicate and the cells were fixed on the indicated days for subsequent staining with crystal violet. The *y* axis represents relative cell numbers measured by attenuance (*D*) at 595 nm. **b**, Transformation assays in WT or *Zbtb7*$^{-/-}$ (Null) MEFs. Oncogene co-infected MEFs were seeded onto soft agar plates and numbers of transformed foci were scored two or three weeks later. **c**, Growth curve of WT MEFs infected with retroviral vectors expressing Pokemon (Pok) along with the indicated oncogenes. Growth curves were generated as described in **a**. Representative pictures of wells stained on the indicated days of culture are also shown. **d**, WT MEFs infected with retroviral vectors expressing Pokemon (Pok) along with the indicated oncogenes were plated onto soft agar plates and transformation assays were performed as in **b**. Error bars in **a**–**d** represent the standard deviation of triplicate wells.

transcriptional modulators, such as E2F1 (refs 19, 20), Bmi-1 (refs 21–26), TBX2, TBX3 (refs 27–29) and Dmp1 (ref. 30), have been reported to regulate the *ARF* promoter (Fig. 2b and Supplementary Fig. 3a).

To determine whether Pokemon would regulate *ARF* gene expression, we first performed transactivation assays with *ARF* promoter constructs fused to luciferase reporters. Pokemon efficiently repressed both $p19^{Arf}$ and $p14^{ARF}$ basal reporter activity in a

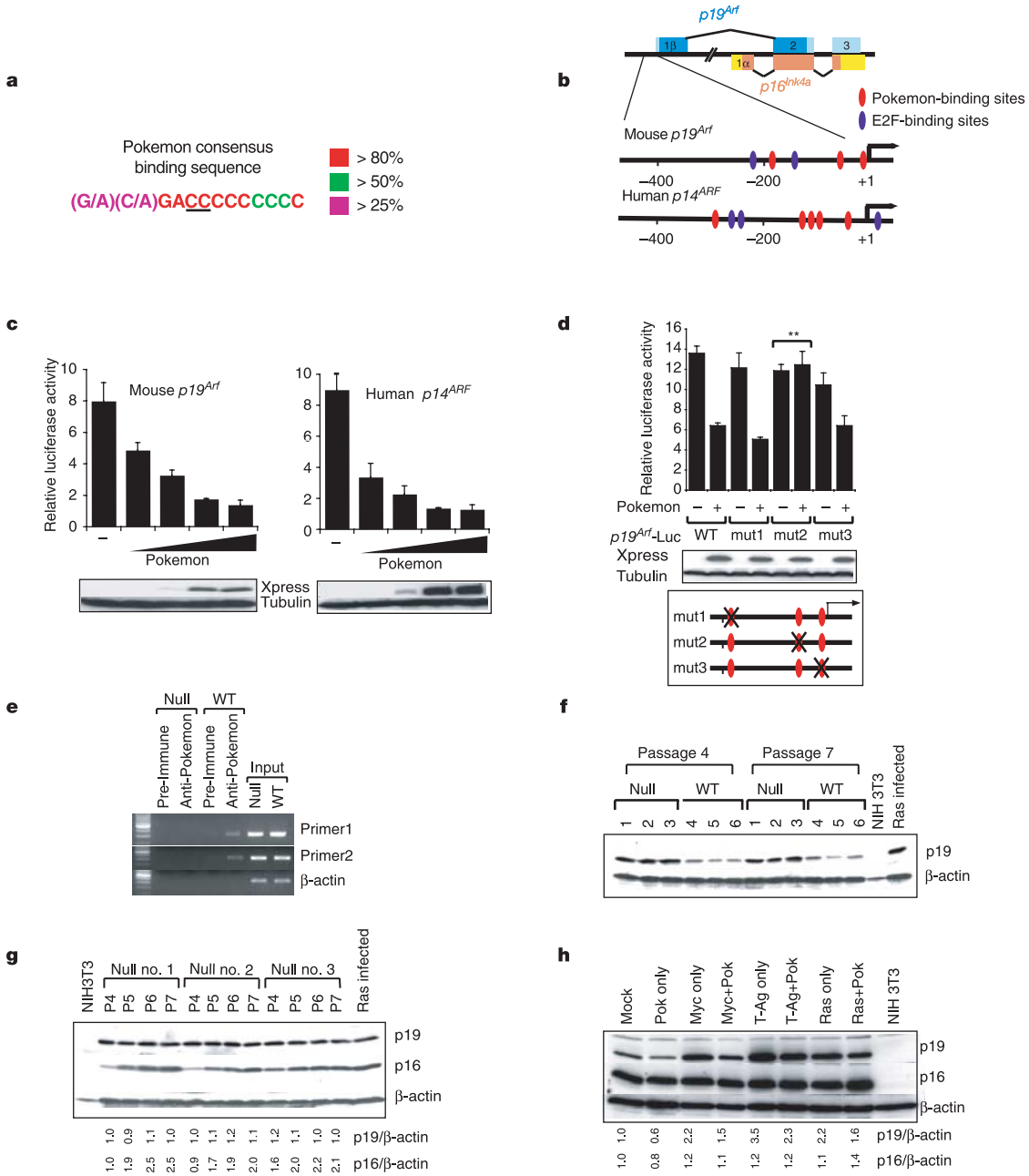

Figure 2 Pokemon is a key *ARF* transcriptional repressor. **a**, Pokemon-binding sequence identified by CAST analysis. The colour code represents the percentage of conserved sequence among pulled-down selected oligonucleotides. The core binding sequence is underlined. **b**, Schematic representation of mouse $p19^{Arf}$ and human $p14^{ARF}$ genes, promoter regions and the relative positions of putative Pokemon-binding sites. **c**, Pokemon represses both human and mouse *ARF* promoter activity. Transrepression assays in NIH3T3 cells transfected with increasing amounts of Pokemon expression vector along with mouse $p19^{Arf}$ and human $p14^{ARF}$ luciferase-based reporters. Pokemon expression levels are shown in the bottom panels. **d**, Identification of an essential Pokemon-binding site in mouse $p19^{Arf}$ promoter. The putative Pokemon-binding sites in mouse $p19^{Arf}$ promoter were mutagenized and subsequently used for reporter assays. Schematic representations of mutated promoter and expression control for the reporter assay are shown (bottom). Pokemon did not repress the promoter activity of mut2 reporter (denoted by asterisk). **e**, ChIP assay in WT and $Zbtb7^{-/-}$ (Null) MEFs. Protein–DNA complexes extracted from MEFs were precipitated either with a preimmune hamster antibody or an anti-Pokemon hamster polyclonal antibody. PCR was performed with primers specific for the $p19^{Arf}$ promoter sequence and primers for amplifying mouse β-actin genomic sequence. Amplified DNA was visualized by agarose-gel electrophoresis. **f**, $p19^{Arf}$ is aberrantly expressed in $Zbtb7^{-/-}$ (Null) MEFs. Western blot analysis of $p19^{Arf}$ in serially passaged MEFs. MEFs were prepared from three independent littermates. **g**, Pokemon is a specific $p19^{Arf}$ repressor. Western blot analysis of $p19^{Arf}$ and $p16^{Ink4a}$ expression in distinct preparations of serially passaged $Zbtb7^{-/-}$ (Null) MEFs. Normalization of $p19^{Arf}$ and $p16^{Ink4a}$ protein levels over β-actin is also shown (bottom). **h**, Pokemon antagonizes oncogene-dependent $p19^{Arf}$ induction. Western blot analysis of $p19^{Arf}$ and $p16^{Ink4a}$ protein expression in WT MEFs infected with retroviral vectors expressing the indicated oncogenes. Error bars in **c** and **d** represent the standard deviation of triplicate wells.

dose-dependent manner (Fig. 2c). We also determined that both the POZ and zinc finger domains are required for this repressive activity (Supplementary Fig. 3b). To identify the Pokemon-binding site essential for Pokemon's repressive activity upon the *p19*^{Arf} promoter, we mutagenized the three putative binding sites in reporter constructs and performed luciferase assays (see Supplementary Fig. 3c). As shown in Fig. 2d, Pokemon was unable to repress mut2 reporter activity, which strongly indicates that the Pokemon-binding site located 50 base pairs upstream from the transcription start site is indispensable for *p19*^{Arf} repression. Furthermore, we found that Pokemon efficiently abrogated E2F1-dependent *ARF* transactivation/de-repression in a dose-dependent manner (Supplementary Fig. 3d, and not shown). We next tested whether Pokemon binds the *p19*^{Arf} promoter *in vivo* by chromatin immunoprecipitation (ChIP) assay and designed two different primer sets to amplify the *p19*^{Arf} promoter region (Supplementary Fig. 3a). In these assays, the anti-Pokemon antibody specifically precipitated *p19*^{Arf} promoter sequences from the extract prepared from WT MEFs but not from *Zbtb7*$^{-/-}$ MEFs (Fig. 2e). Furthermore, anti-Pokemon antibody was unable to precipitate β-actin genomic sequences, which indicates that Pokemon binding might be specific for the *p19*^{Arf} promoter. ChIP assays were also performed in transformed MEFs, confirming that Pokemon also binds to the *p19*^{Arf} promoter under transformed conditions (not shown). Thus, Pokemon can bind to the *p19*^{Arf} promoter *in vivo* and repress its activity.

The effect of *Zbtb7* inactivation on *p19*^{Arf} expression was then evaluated. p19^{Arf} protein levels were remarkably higher in *Zbtb7*$^{-/-}$ MEFs starting from passage four, when p19^{Arf} is normally induced due to culture shock[14] (Fig. 2f). *p19*^{Arf} upregulation also occurred at the mRNA level as indicated by real-time polymerase chain reaction (PCR) analysis (Supplementary Fig. 3e). The *Ink4a-Arf* locus encodes two tumour suppressors, p16^{Ink4a} and p19^{Arf}, which are homologous to human p16^{INK4A} and p14^{ARF}, respectively[31]. Both genes are able to induce cellular senescence in response to oncogenic stimuli, and their functional loss is frequently observed in human cancers[32,33]. Interestingly, in *Zbtb7*$^{-/-}$ MEFs, only p19^{Arf} but not p16^{Ink4a} was constitutively upregulated, whereas gradual increases in p16^{Ink4a} levels with passaging occurred comparably in *Zbtb7*$^{-/-}$ and WT MEFs (Fig. 2g, and not shown). Furthermore, Pokemon was unable to repress the mouse *p16*^{Ink4a} promoter activity as revealed by luciferase assay (Supplementary Fig. 3f), which also supports the notion that Pokemon is a specific repressor for *p19*^{Arf} but not for *p16*^{Ink4a}. In complete agreement with these findings, *p53* (a key downstream target gene of *p19*^{Arf}) was also found overexpressed in *Zbtb7*$^{-/-}$ MEFs (Supplementary Fig. 3g).

We then examined whether Pokemon overexpression would repress p19^{Arf} expression levels and whether this would also occur in transforming conditions when p19^{Arf} is induced in primary cells. Indeed, Pokemon overexpression invariably resulted in decreased p19^{Arf} levels under these conditions (Fig. 2h). p19^{Arf} levels were also examined in protein extracts obtained from transformed colonies in these oncogene combinations. p19^{Arf} and Pokemon protein

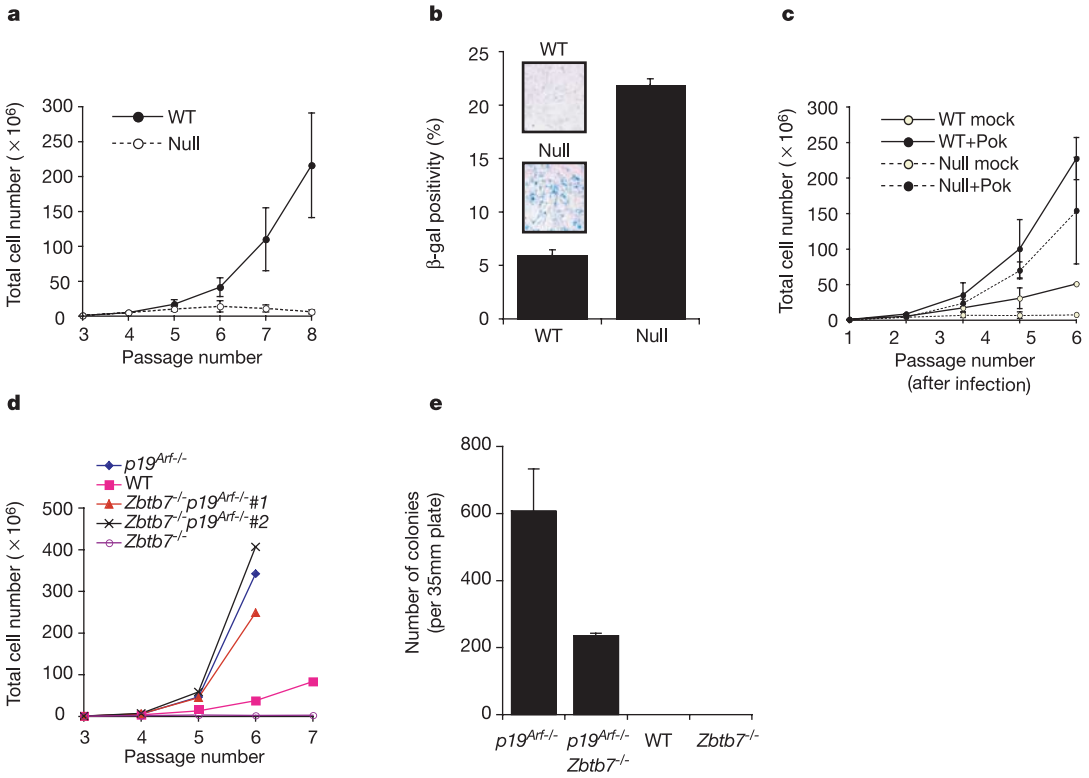

Figure 3 *p19*^{Arf} loss reverts premature senescence and refractoriness to oncogenic transformation in *Zbtb7*$^{-/-}$ MEFs. **a**, Growth curves from WT and *Zbtb7*$^{-/-}$ (Null) MEFs seeded and passaged by following a 3T9 protocol. Each time point represents the mean ± s.d. of total cumulative cell number from three independent WT and null MEF cultures. **b**, Senescence assays in WT and null MEFs. The *y* axis represents the percentage of β-galactosidase-positive cells (mean and s.d.) from three independent WT and null MEFs cultures at passage six. A representative result of three independent experiments is shown. **c**, Pokemon add-back rescues the premature senescence phenotype in *Zbtb7*$^{-/-}$ MEFs. Growth curves from WT and *Zbtb7*$^{-/-}$ (Null) MEFs that were either Pokemon-infected or mock-infected. Each time point represents the mean ± s.d. of total cumulative cell number from two independent WT and null infected MEF cultures. **d**, *p19*^{Arf} inactivation rescues the premature senescence phenotype in *Zbtb7*$^{-/-}$ MEFs. Growth curves of MEFs generated from embryos obtained from *Zbtb7*$^{+/-}$*p19*$^{Arf+/-}$ intercrosses are shown. MEFs of various genotypes were derived from littermates. Cumulative cell number was counted as described in **a**. **e**, *p19*^{Arf} inactivation overcomes the refractoriness to oncogenic transformation observed in *Zbtb7*$^{-/-}$ MEFs. WT, *Zbtb7*$^{-/-}$, *p19*$^{Arf-/-}$ and *Zbtb7*$^{-/-}$*p19*$^{Arf-/-}$ MEFs obtained as described in **d** were infected with oncogenic *ras*, and soft agar transformation assays were performed as described previously.

expression levels were inversely correlated, whereas $p16^{Ink4a}$ expression was not affected (not shown). These data therefore demonstrate that Pokemon is an important and selective repressor of $p19^{Arf}$ expression.

Loss of *Arf* rescues *Zbtb7*$^{-/-}$ MEF transformability

Accumulation of $p19^{Arf}$ correlates with the onset of cellular senescence in MEFs after culture shock[14]. In full agreement with the finding that Pokemon represses $p19^{Arf}$ expression and that $p19^{Arf}$ upregulation is observed in *Zbtb7*$^{-/-}$ MEFs from about passage four, *Zbtb7*$^{-/-}$ MEFs proliferated normally until this passage number and their proliferative capacity rapidly declined at later passages (Fig. 3a). This was accompanied by a marked increase in cellular senescence as demonstrated by staining for the senescence marker β-galactosidase[34] (Fig. 3b). As expected, these cell growth defects were fully rescued by Pokemon add-back. In addition, Pokemon overexpression further enhanced the proliferative potential of WT MEFs (Fig. 3c).

We next tested whether *p19*^{Arf} loss could rescue the proliferative defect and premature senescence phenotype observed in *Zbtb7*$^{-/-}$ MEFs. To this end, *Zbtb7* and *p19*^{Arf} double-knockout MEFs (*Zbtb7*$^{-/-}$*p19*$^{Arf-/-}$ MEFs) were established from double-mutant embryos. Indeed, the growth defects in *Zbtb7*$^{-/-}$ MEFs were fully reverted by *p19*^{Arf} loss, and *Zbtb7*$^{-/-}$*p19*$^{Arf-/-}$ MEFs proliferated indistinguishably from *p19*$^{Arf-/-}$ MEFs (Fig. 3d). Furthermore, *p19*^{Arf} inactivation also reverted the refractoriness to oncogenic transformability observed in *Zbtb7*$^{-/-}$ MEFs. *Zbtb7*$^{-/-}$*p19*$^{Arf-/-}$ MEFs were susceptible to transformation by oncogenic *ras* alone (Fig. 3e).

Pokemon is oncogenic *in vivo*

To determine whether Pokemon would act as a genuine proto-oncogene *in vivo*, we generated a transgenic mouse model in which Pokemon is overexpressed in immature T and B lymphoid lineage cells taking advantage of an *lck*Eμ enhancer/promoter transgenic construct[35] (Fig. 4a). Positive transgenic founders were identified and the expression levels of the transgene in F_1 mice from the various founders were assessed by semiquantitative polymerase chain reaction with reverse transcription (RT–PCR) from splenocyte RNA (Supplementary Fig. 4a). We selected two of the highest-expressing lines (numbers 16 and 26) and the F_1 and F_2 generations of each line (litters obtained by intercross with negative mice) were used for further study.

Strikingly, both transgenic lines developed aggressive tumours. The hallmark of the disease in these *lck*Eμ-Pokemon mice was massive thymic enlargement, accompanied by lymphadenopathy, splenomegaly, hepatomegaly and tumour infiltration into bone marrow (Fig. 4b). Histopathological examinations of the tumours revealed that the thymus and lymph node architecture was completely effaced and showed a starry-sky pattern with tingible-body macrophages. The lymphomas contained a monotonous population of immature lymphoid cells. The spleen showed expansion of the white pulp and effacement and infiltration of the red pulp by tumour cells. The liver showed prominent periportal, lobular and sinusoidal infiltration by tumour cells (Fig. 4c).

To further characterize the phenotype of these lymphomas, we performed flow cytometry analysis. The lymphomas typically showed an immature T-cell immunophenotype ($CD3^+$, $CD4^{++}$, $CD8^{++}$ $CD44^{++}$, $CD25^-$; Fig. 4d). Furthermore, Wright–Giemsa

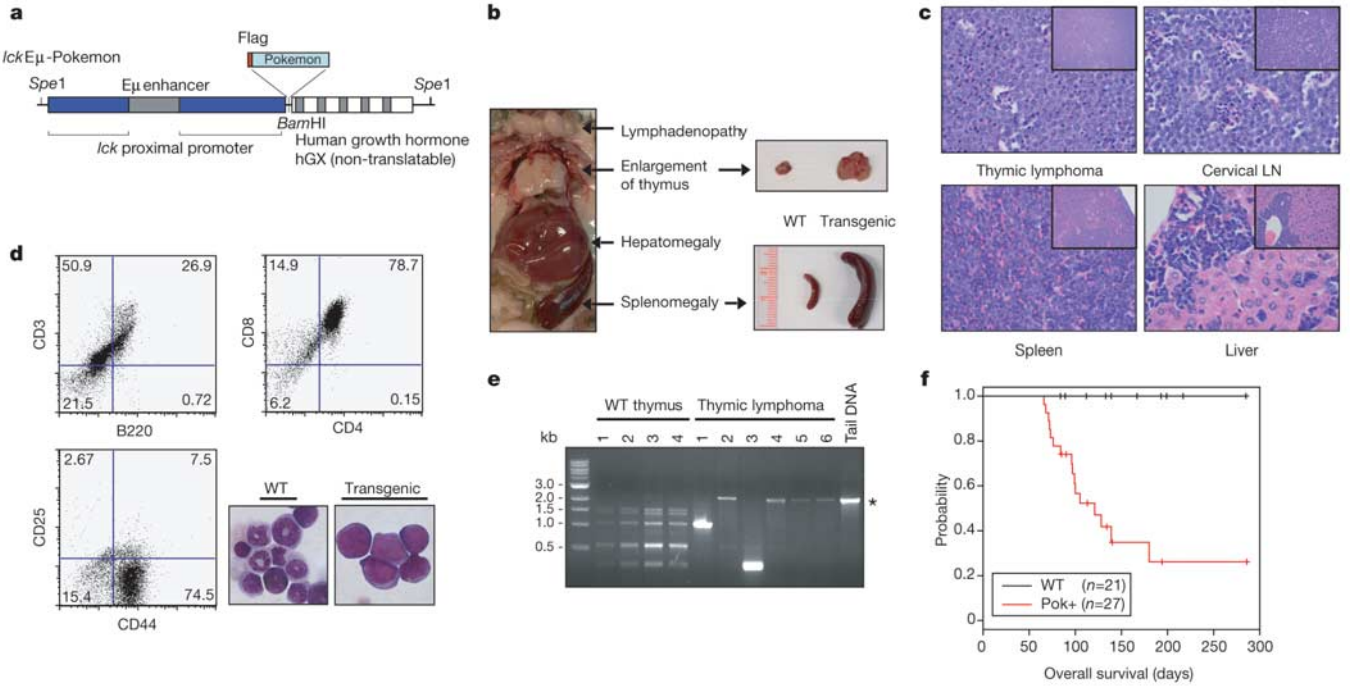

Figure 4 Pokemon transgenic mice develop pre-T LBL. **a**, Diagram of transgenic construct used to overexpress Flag-tagged Pokemon in B lymphocytes and immature T lymphocytes[35]. **b**, The left panel shows an image of a 3.5-month-old transgene-positive female from the no. 26 line, which showed enlargement of thymus with splenomegaly, hepatomegaly and lymphadenopathy. WT littermate thymus and spleen are compared with enlarged thymus and spleen developed by transgenic mice in the upper and lower right panels respectively. **c**, Sections from an *lck*Eμ-Pokemon thymic tumour, enlarged cervical lymph node, spleen and liver stained with haematoxylin and eosin. Infiltration of the spleen and liver can be clearly seen. Both high-power (magnification ×400) and low-power (insets, magnification ×40) views are shown. **d**, Flow cytometry analysis of an *lck*Eμ-Pokemon thymic lymphoma for the markers indicated (B220/CD3, CD4/CD8 and CD44/CD25) showing an immature T-cell immunophenotype ($CD3^+$, $CD4^{++}$, $CD8^{++}$ $CD44^{++}$, $CD25^-$). The lower right panels show images of Wright–Giemsa stained cells from bone marrow cytospins of a WT control mouse and a transgene-positive mouse in which the marrow had been completely infiltrated by blasts. **e**, Thymic lymphomas of *lck*Eμ-Pokemon mice were monoclonal in origin. The image shows an analysis of Dβ1-to-Jβ1 rearrangement at the T-cell antigen receptor-β locus by PCR, performed as described[39]. DNA samples from thymocytes of four WT mice and cells from six *lck*Eμ-Pokemon thymic lymphomas were analysed together with a tail DNA control. The asterisk shows the germline configuration. **f**, Kaplan–Meir plot of overall survival of *lck*Eμ-Pokemon mice from the no. 26 founder line against WT control littermates.

staining of the bone marrow tumour cells showed large lymphoblasts with round nuclei, fine chromatin and scanty cytoplasm, which is fully consistent with a mouse precursor T-cell lymphoblastic lymphoma/leukaemia (pre-T LBL)[36] (Fig. 4d, bottom right). Taking advantage of a specific anti-Pokemon monoclonal antibody 13E9 (Supplementary Fig. 4b), immunohistochemistry of lymphoma sections showed intense nuclear positivity for Pokemon (Supplementary Fig. 4c). However, in normal thymus, Pokemon is expressed mainly in medullary epithelial cells and Hassle's corpuscles, which are negative for the T-cell linage marker CD3 and positive for the epithelial cell marker cytokeratin AE1:AE3 (Supplementary Fig. 5a, d). In addition, lymphomas were highly positive for terminal deoxynucleotidyl transferase, a diagnostic marker for lymphoblastic lymphoma/leukaemia (Supplementary Fig. 4c)[37,38]. The increased Pokemon protein expression in thymic lymphomas was also confirmed by western blot analysis (Supplementary Fig. 4d). To examine whether the lymphomas were monoclonal in origin, we extracted DNA from six different thymic lymphomas and analysed Dβ1-to-Jβ1 rearrangement of the T-cell antigen receptor-β locus. Four thymic DNA samples from WT mice were used as controls. As shown in Fig. 4e, either a single non-rearranged (or rearranged in other D and J elements) band or a predominant single rearranged band was amplified in lymphoma DNA, whereas PCR products from the four WT thymic DNA demonstrated five possible rearranged and one germline non-rearranged band, as described previously[39]. These data indicate that the *lck*Eμ-Pokemon lympho-

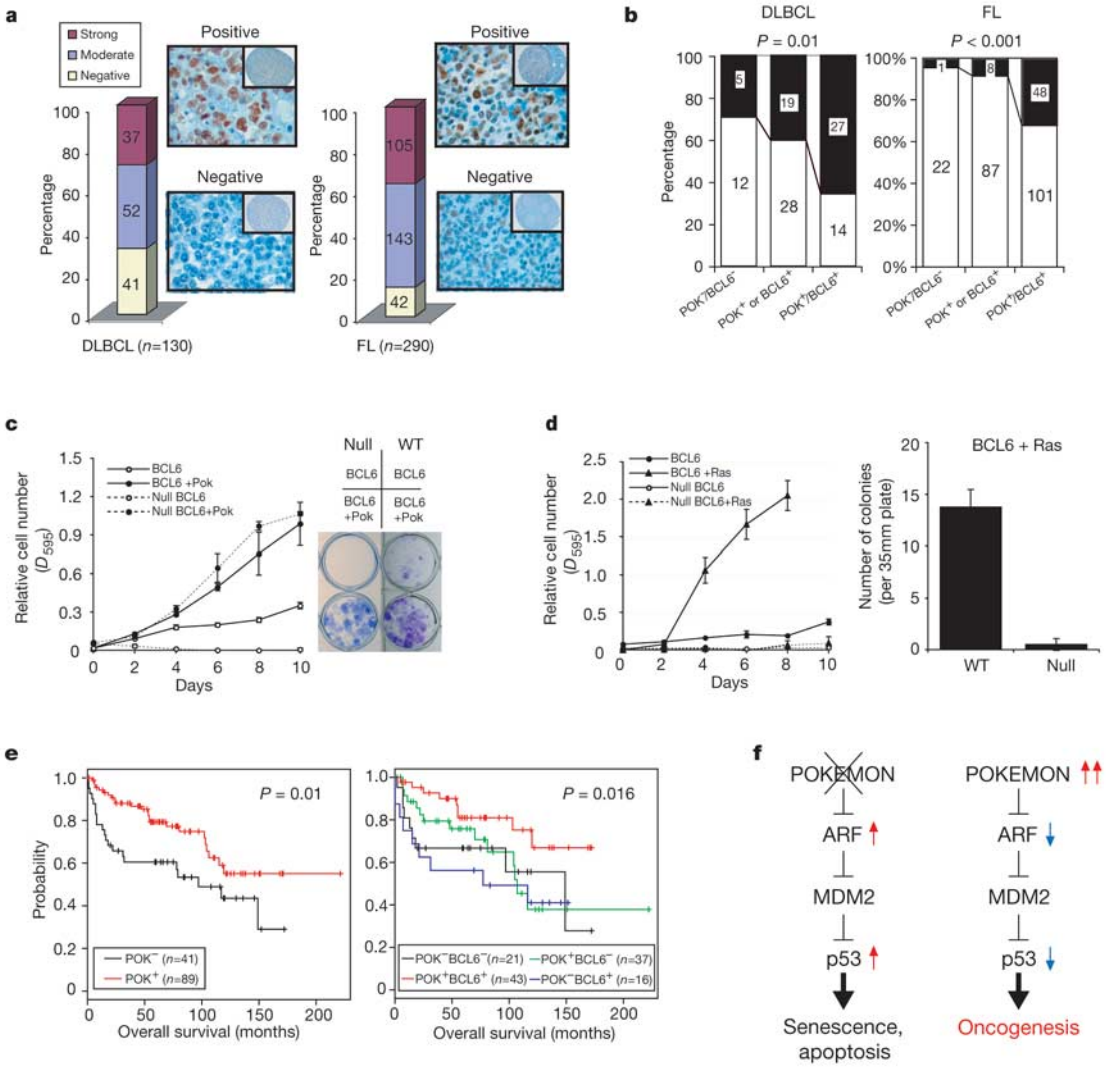

Figure 5 Cooperative roles of Pokemon and BCL6 in lymphomagenesis. **a**, TMA analysis of Pokemon expression in DLBCL and FL clinical samples. Bar graphs show the percentage of Pokemon positivity among samples. Colours indicate levels of Pokemon expression. Absolute numbers of tumours are indicated. Representative pictures of samples positive and negative for Pokemon expression are also shown. **b**, Percentage of Ki-67-positive and Ki-67-negative samples according to Pokemon (Pok) and BCL6 expression pattern. Ki-67-positive and Ki-67-negative samples are represented as black and white bars, respectively. The *y* axis represents the percentage of positive and negative cases among each group. Absolute numbers are also indicated. **c**, Pokemon (Pok) is required for BCL6-dependent cell immortalization. Left, growth curves from WT and *Zbtb7*$^{-/-}$ (Null) MEFs after infection with a *BCL6* retroviral vector. Relative cell numbers were measured as described in Fig. 1a. Right, representative pictures of cell cultures stained with crystal violet on day 10. BCL6 and Pokemon did not confer full transforming capability to MEFs (not shown). **d**, Left, growth curves from WT and *Zbtb7*$^{-/-}$ (Null) MEFs infected with either *BCL6* alone or *BCL6* together with oncogenic *ras*. Right, transformation assays in soft agar in WT and *Zbtb7*$^{-/-}$ (Null) MEFs. *BCL6* and *H-ras*^{V12} co-infected MEFs of the indicated genotypes were plated onto soft agar plates and the numbers of transformed foci were scored after three weeks. Error bars in **c** and **d** represent the standard deviation of triplicate wells. **e**, Pokemon expression predicts better clinical outcome in DLBCL. Left, overall survival Kaplan–Meier curves of DLBCL cases stratified according to Pokemon-positive and Pokemon-negative expression. Numbers of cases are also indicated. Right, overall survival Kaplan–Meier curves of DLBCL cases stratified according to Pokemon and BCL6 coexpression patterns. Numbers of cases are also indicated. **f**, Proposed model for the role of Pokemon in oncogenesis. Abrogation of Pokemon function leads to cell cycle arrest, cellular senescence and apoptosis, and hence could be exploited for cancer therapy.

mas were monoclonal. These lymphomas were fatal. Specifically, 16 of 27 transgene-positive mice from the number 26 line (the line expressing Pokemon most) developed tumours, and these mice either died or became terminally ill (and hence were killed) between 9 and 40 weeks of age (median 14 weeks) (Fig. 4f). Transgenic mice from the number 16 line also gave rise to pre-T LBL, but at a lower penetrance (4 of 18 mice).

Aberrant Pokemon expression in human cancer

As Pokemon expression proved essential for cellular transformation and this transcription factor is oncogenic when overexpressed both *in vitro* and *in vivo*, we analysed the levels of Pokemon expression in human cancers performing tissue microarray analysis (TMA)[40] with an anti-Pokemon monoclonal antibody 13E9. We first analysed human T-cell and B-cell lymphomas because *lck*Eμ-Pokemon mice developed T-cell lymphomas and Pokemon is normally coexpressed with BCL6 in the B-cell within the germinal centre (Supplementary Fig. 5b, c, and not shown), and might therefore cooperate with BCL6 in lymphomagenesis. We initially performed TMA on small cohorts of T-cell and B-cell lymphoma cases (Supplementary Fig. 6a, b). Interestingly, Pokemon is highly expressed in a subset of T-cell lymphomas, although Pokemon was barely detectable in normal human thymic CD3-positive cells. Furthermore, Pokemon is strongly expressed in diffuse large B-cell lymphoma (DLBCL) and follicular lymphoma (FL), in whose pathogenesis BCL6 is known to be involved.

We subsequently analysed and scored 130 cases of DLBCL and 290 cases of FL for Pokemon protein expression levels (for patient's clinical and immunohistochemical features, see Supplementary Tables 1 and 2 and Supplementary Fig. 6c). Pokemon was highly expressed in 25–35% and moderately expressed in 40–50% of both DLBCL and FL clinical samples (Fig. 5a).

With the use of DNA microarray and TMA analysis, it has recently been proposed that DLBCL can be divided into prognostically significant subgroups with a germinal-centre B-cell-like (GCB) and an activated B-cell-like phenotype[41–43]. We therefore scored and analysed the expression of GCB markers in our DLBCL cohort and correlated these with Pokemon expression levels. Pokemon expression was not significantly correlated with the GCB phenotype, although Pokemon is expressed in the germinal centre in normal reactive tonsil (Supplementary Table1).

Interestingly, the vast majority of BCL6-positive DLBCL and FL were found to be Pokemon positive (Supplementary Fig. 6d). In addition, lymphomas positive for both proteins displayed a higher proliferative index than single-negative or double-negative tumours, as revealed by Ki-67 staining, indicating a possible functional cooperation between Pokemon and BCL6 in tumorigenesis (Fig. 5b). BCL6 can immortalize primary cells and fully transform them in cooperation with oncogenic *ras*[44]. Pokemon proved essential for BCL6 immortalizing and transforming activities in MEFs (Fig. 5c, d). Pokemon overexpression not only rescued these defects in *Zbtb7*$^{-/-}$ cells, but also markedly potentiated the growth-promoting activity of BCL6 (Fig. 5c). This cooperative crosstalk between Pokemon and BCL6 in tumorigenesis indicated, in turn, that Pokemon expression and/or Pokemon/BCL6 coexpression might identify a specific lymphoma subtype and possibly predict its clinical outcome. Strikingly, Pokemon positivity was predictive of better overall survival in DLBCL (Fig. 5e, left). Furthermore, Pokemon and BCL6 double positivity predicted an even better clinical outcome for overall survival (Fig. 5e, right).

Discussion

We have demonstrated that Pokemon expression levels are critical determinants of the cellular response to oncogenic transformation. We show that the function of this novel member of the POK family of transcriptional repressors is necessary for oncogenic transformation whereas, conversely, Pokemon can act as a genuine proto-oncogene when overexpressed (Fig. 5f). Importantly, taking advantage of a transgenic mouse model, we demonstrate that Pokemon can indeed act as a proto-oncogene *in vivo*.

We identify Pokemon as a potent transcriptional repressor of the $p19^{Arf}$ tumour suppressor gene. Pokemon is, to our knowledge, the first *ARF*-specific transcriptional repressor to be identified. Furthermore, $p19^{Arf}$ inactivation rescued the refractoriness to oncogenic transformation of *Zbtb7*$^{-/-}$ cells. Taken together, these data strongly indicate that, at least in certain cell types, one of the main oncogenic functions of Pokemon consists of its ability to repress $p19^{Arf}$ expression. Interestingly, real-time RT–PCR analysis of a cohort of DLBCL cases (n=37) revealed that high *Pokemon* gene expression is generally correlated with low expression of the $p14^{ARF}$ gene (Supplementary Fig. 6f). Our findings underscore the potential importance of *ARF* suppression in human tumorigenesis.

We show that Pokemon is expressed at very high levels in a subset of human lymphomas. TMA analyses in breast, lung, colon, prostate and bladder carcinomas also reveal high levels of Pokemon expression in a subset of these tumours (T.M. and P.P.P., unpublished data). In this respect, it is worth noting that the genomic region where the *ZBTB7* gene resides (chromosome 19p13.3) is a hotspot for chromosomal translocations (CGAP; http://cgap.nci.nih.gov/Chromosomes). We show that Pokemon expression or its coexpression with BCL6 in lymphoma predicts clinical outcome. This is in keeping with the fact that Pokemon is required for BCL6 oncogenic activity, and that high expression of potent proto-oncogenes such as BCL6 and LMO2 also identifies cohorts of patients who respond better to current treatment modalities[41,43,45]. Cooperative tumorigenesis between these two proto-oncogenes could be exerted through distinct transcriptional programmes or pathways[46], but also through co-regulation of common target genes in view of their ability to interact physically. In this respect, it is of interest that BCL6 has recently been reported to repress *p53* expression directly[47].

Our findings provide a further rational for transcription-based therapeutic modalities and identify *Pokemon* as an important target for therapy on the basis of its key role in oncogenesis. □

Methods

Growth curves, transformation and senescence assays

MEFs were prepared from embryos at 13.5 days post coitus. MEFs at passage one or two were used for all experiments. Growth curves after oncogene infections were generated by seeding 3,000 cells (per well) in 12-well plates in triplicate[48]. For transformation assays, 5×10^4 cells were resuspended in 1.5 ml complete Dulbecco's modified Eagle's medium containing 0.3% agarose and seeded into 35-mm plates containing a 3-ml layer of solidified 0.6% agar in complete medium. Foci were scored two or three weeks later. For growth curves of unmanipulated MEFs, 9×10^5 cells were plated in 10-cm dishes and passaged every fourth day. For senescence assays, β-galactosidase-positive cells were scored at passage six in accordance with the manufacturer's specification (Senescence detection kit; Oncogene). The Rat1 MycEr™ cells were kindly provided by G. I. Evan. The mock-infected (pWZL-Hygro) cells and the Pokemon-infected (pWZL-Flag-Pokemon) cells were generated by us. After 24 h of serum deprivation, Myc-induced apoptosis was subsequently triggered by the addition of 100 nM 4-hydroxytamoxifen (Sigma) in medium containing 0.1% serum[16], and apoptotic cells were scored with the trypan blue exclusion method on the indicated days.

Molecular analysis

Western blotting was performed in accordance with the standard protocol with the following antibodies: E1A (M58; NeoMarkers), T-Ag (SV40 Ab-1; NeoMarkers), Myc (no. 06-340; Upstate), Ras (Ab-3; Oncogene), Xpress (Invitrogen), $p19^{Arf}$ (Ab-1 PC435 lot no. D18714-1; Oncogene), $p16^{Ink4a}$ (M-156; Santa Cruz), p53 (Ab-7; Oncogene) and BCL6 (N-3; Santa Cruz). Anti-Pokemon hamster monoclonal antibody (clone 13E9) was raised against a peptide derived from the Pokemon N-terminal region (amino acids 1–20, MAGGVDGPIGIPFPDHSSDI), fully conserved between human and mouse proteins. Loading was assessed by β-actin (A-5316; Sigma), α-tubulin (B-5-1-2; Sigma) or Hsp-90 (no. 610419; BD). CAST analysis and EMSA were performed as described[18]. For reporter assays, 10^5 NIH 3T3 cells per well were plated into 12-well plates in triplicate 16 h before transfection, and cells were transfected with Lipofectamine 2000. At 24 h after transfection, cells were assayed with a dual luciferase assay kit (Promega).

Plasmids

Mouse *Zbtb7* complementary DNA was amplified by PCR from C57BL/6 mouse bone marrow total cDNA and subcloned into the pcDNA3.1His vector (containing the Xpress

tag; Invitrogen), pSG5 vector (with Flag sequence; Stratagene), pWZL-Hygro and MSCV-PIG vectors (Puro-IRES-GFP, provided by S. W. Lowe). Pokemon deletion mutant constructs used for reporter assays (pcDNA3.1His-POZ, ΔPOZ, Zn and ΔZn) were generated from the pcDNA3.1His-Pokemon vector. Retroviral vectors, expression vectors and luciferase constructs were gifts from A. Koff (pWZL-Hygro-human-c-Myc and pSG5-T-Ag), R. Bernards (pBabe-Hygro-BCL6), S. W. Lowe (pBabe-puro-H-*ras*V12 and pWZL-Hygro-E1A), W. Kaelin (pRc-CMV-HA-E2F1); S. W. Hiebert (human $p14^{ARF}$-luciferase reporter plasmid), M. F. Roussel (mouse $p19^{Arf}$-luciferase reporter plasmid), B. A. Mock (mouse $p16^{Ink4a}$-luciferase reporter plasmid) and R. M. Perlmutter (p1026X vector). Mutated $p19^{Arf}$-luciferase reporters were constructed by using a QuikChange Mutagenesis Kit (Stratagene). pWZL-Hygro-T-Ag was generated from the pSG5-T-Ag vector. pWZL-Hygro-H-*ras*V12 was generated from the pBabe-puro-H-*ras*V12 vector. 3POKBB-Luc was constructed by insertion of three copies of the Pokemon-binding sequence (5′-GGTTAAAAGACCCCTCCCCGAATTCGGATC-3′) into a luciferase reporter vector TK-LUC from R. Dalla-Favera.

Generation of $Zbtb7^{-/-}p19^{Arf-/-}$ mutants

$Zbtb7^{+/-}$ mice and $p19^{Arf+/-}$ mice (provided by C. J. Sherr) were crossed to generate $Zbtb7^{+/-}p19^{Arf+/-}$ double-heterozygous mice, which were subsequently intercrossed to generate $Zbtb7^{-/-}p19^{Arf-/-}$ embryos and MEFs along with WT and single-mutant littermates.

Generation and characterization of *lck*Eμ-Pokemon mice

The Flag-Pokemon transgene was produced by ligating the 1.7-kilobase Flag-Pokemon cDNA sequence (from pSG5 Flag-Pokemon vector) into the *Bam*H1 cloning site of the p1026X vector[35]. For generating transgenic mice, a purified *Spe*1 fragment containing *lck*Eμ-Pokemon was injected into fertilized (C57BL/6J × CBA/J) F_2 eggs at the MSKCC Transgenic Mouse Core Facility. Transgenic founders were detected by Southern blotting of tail DNA with a Flag-Pokemon cDNA fragment (generated from pSG5 Flag-Pokemon) as a probe. Positive founders were intercrossed with negative founders to establish F_1 generations, and the colony of two highest copy founder lines (nos 16 and 26, revealed by Southern blotting and RT–PCR) were expanded and used for further characterization. To examine the monoclonality of thymic lymphomas, DNA was extracted from WT thymus and thymic lymphomas and the D-to-J rearrangements of the T-cell antigen receptor-β locus were analysed as described previously, using primers 1 and 4 (ref. 39).

TMA analysis

The study cohort comprised 130 DLBCL and 290 FL biopsies consecutively ascertained at the Memorial Sloan-Kettering Cancer Center (MSKCC) between 1984 and 2000. Patient anonymity was ensured and the study received a waiver by the Institutional Review Board. All DLBCL biopsies were obtained at their first evaluation at MSKCC and all DLBCL patients received an anthracyclin-based chemotherapy regimen. The initial histological diagnosis was based on haematoxylin–eosin staining and immunophenotyping results. Biopsies were reviewed and reclassified histologically in accordance with the World Health Organization classification[38]. TMAs were constructed and stained in the Pathology and Molecular Cytology Core Facilities as described previously[49]. Further detailed information, including staining conditions and antibody dilutions, is described in Supplementary Methods.

Received 17 September; accepted 18 November 2004; doi:10.1038/nature03203.

1. Lin, R. J. *et al.* Role of the histone deacetylase complex in acute promyelocytic leukaemia. *Nature* **391,** 811–814 (1998).
2. Melnick, A. *et al.* Critical residues within the BTB domain of PLZF and Bcl-6 modulate interaction with corepressors. *Mol. Cell. Biol.* **22,** 1804–1818 (2002).
3. Barna, M., Hawe, N., Niswander, L. & Pandolfi, P. P. Plzf regulates limb and axial skeletal patterning. *Nature Genet.* **25,** 166–172 (2000).
4. Ye, B. H. *et al.* The BCL-6 proto-oncogene controls germinal-centre formation and Th2-type inflammation. *Nature Genet.* **16,** 161–170 (1997).
5. Adhikary, S. *et al.* Miz1 is required for early embryonic development during gastrulation. *Mol. Cell. Biol.* **23,** 7648–7657 (2003).
6. Carter, M. G. *et al.* Mice deficient in the candidate tumor suppressor gene Hic1 exhibit developmental defects of structures affected in the Miller–Dieker syndrome. *Hum. Mol. Genet.* **9,** 413–419 (2000).
7. Chen, W. Y. *et al.* Heterozygous disruption of Hic1 predisposes mice to a gender-dependent spectrum of malignant tumors. *Nature Genet.* **33,** 197–202 (2003).
8. Chen, Z. *et al.* Fusion between a novel Kruppel-like zinc finger gene and the retinoic acid receptor-alpha locus due to a variant t(11;17) translocation associated with acute promyelocytic leukaemia. *EMBO J.* **12,** 1161–1167 (1993).
9. Ye, B. H. *et al.* Alterations of a zinc finger-encoding gene, BCL-6, in diffuse large-cell lymphoma. *Science* **262,** 747–750 (1993).
10. Davies, J. M. *et al.* Novel BTB/POZ domain zinc-finger protein, LRF, is a potential target of the LAZ-3/BCL-6 oncogene. *Oncogene* **18,** 365–375 (1999).
11. Kukita, A. *et al.* Osteoclast-derived zinc finger (OCZF) protein with POZ domain, a possible transcriptional repressor, is involved in osteoclastogenesis. *Blood* **94,** 1987–1997 (1999).
12. Pessler, F., Pendergrast, P. S. & Hernandez, N. Purification and characterization of FBI-1, a cellular factor that binds to the human immunodeficiency virus type 1 inducer of short transcripts. *Mol. Cell. Biol.* **17,** 3786–3798 (1997).
13. Weinberg, R. A. The cat and mouse games that genes, viruses, and cells play. *Cell* **88,** 573–575 (1997).
14. Zindy, F. *et al.* Myc signaling via the ARF tumor suppressor regulates p53-dependent apoptosis and immortalization. *Genes Dev.* **12,** 2424–2433 (1998).
15. Serrano, M., Lin, A. W., McCurrach, M. E., Beach, D. & Lowe, S. W. Oncogenic ras provokes premature cell senescence associated with accumulation of p53 and p16INK4a. *Cell* **88,** 593–602 (1997).
16. Evan, G. I. *et al.* Induction of apoptosis in fibroblasts by c-myc protein. *Cell* **69,** 119–128 (1992).
17. de Stanchina, E. *et al.* E1A signaling to p53 involves the p19(ARF) tumor suppressor. *Genes Dev.* **12,** 2434–2442 (1998).
18. Wright, W. E., Binder, M. & Funk, W. Cyclic amplification and selection of targets (CASTing) for the myogenin consensus binding site. *Mol. Cell. Biol.* **11,** 4104–4110 (1991).
19. Bates, S. *et al.* $p14^{ARF}$ links the tumour suppressors RB and p53. *Nature* **395,** 124–125 (1998).
20. Rowland, B. D. *et al.* E2F transcriptional repressor complexes are critical downstream targets of p19(ARF)/p53-induced proliferative arrest. *Cancer Cell* **2,** 55–65 (2002).
21. Jacobs, J. J. L., Kieboom, K., Marino, S., DePinho, R. A. & van Lohuizen, M. The oncogene and Polycomb-group gene *bmi-1* regulates cell proliferation and senescence through the *ink4a* locus. *Nature* **397,** 164–168 (1999).
22. Jacobs, J. J. *et al.* Bmi-1 collaborates with c-Myc in tumorigenesis by inhibiting c-Myc-induced apoptosis via INK4a/ARF. *Genes Dev.* **13,** 2678–2690 (1999).
23. Smith, K. S. *et al.* Bmi-1 regulation of INK4A-ARF is a downstream requirement for transformation of hematopoietic progenitors by E2a-Pbx1. *Mol. Cell* **12,** 393–400 (2003).
24. Kranc, K. R. *et al.* Transcriptional coactivator Cited2 induces Bmi1 and Mel18 and controls fibroblast proliferation via Ink4a/ARF. *Mol. Cell. Biol.* **23,** 7658–7666 (2003).
25. Kim, J. H. *et al.* The Bmi-1 oncoprotein is overexpressed in human colorectal cancer and correlates with the reduced p16INK4a/p14ARF proteins. *Cancer Lett.* **203,** 217–224 (2004).
26. Vonlanthen, S. *et al.* The bmi-1 oncoprotein is differentially expressed in non-small cell lung cancer and correlates with INK4A-ARF locus expression. *Br. J. Cancer* **84,** 1372–1376 (2001).
27. Jacobs, J. J. *et al.* Senescence bypass screen identifies TBX2, which represses Cdkn2a (p19(ARF)) and is amplified in a subset of human breast cancers. *Nature Genet.* **26,** 291–299 (2000).
28. Lingbeek, M. E., Jacobs, J. J. & van Lohuizen, M. The T-box repressors TBX2 and TBX3 specifically regulate the tumor suppressor gene p14ARF via a variant T-site in the initiator. *J. Biol. Chem.* **277,** 26120–26127 (2002).
29. Brummelkamp, T. R. *et al.* TBX-3, the gene mutated in Ulnar-Mammary Syndrome, is a negative regulator of p19ARF and inhibits senescence. *J. Biol. Chem.* **277,** 6567–6572 (2002).
30. Inoue, K., Roussel, M. F. & Sherr, C. J. Induction of ARF tumor suppressor gene expression and cell cycle arrest by transcription factor DMP1. *Proc. Natl Acad. Sci. USA* **96,** 3993–3998 (1999).
31. Quelle, D. E., Zindy, F., Ashmun, R. A. & Sherr, C. J. Alternative reading frames of the INK4a tumor suppressor gene encode two unrelated proteins capable of inducing cell cycle arrest. *Cell* **83,** 993–1000 (1995).
32. Sherr, C. J. & McCormick, F. The RB and p53 pathways in cancer. *Cancer Cell* **2,** 103–112 (2002).
33. Lowe, S. W. & Sherr, C. J. Tumor suppression by Ink4a-Arf: progress and puzzles. *Curr. Opin. Genet. Dev.* **13,** 77–83 (2003).
34. Dimri, G. P. *et al.* A biomarker that identifies senescent human cells in culture and in aging skin *in vivo*. *Proc. Natl Acad. Sci. USA* **92,** 9363–9367 (1995).
35. Iritani, B. M., Forbush, K. A., Farrar, M. A. & Perlmutter, R. M. Control of B cell development by Ras-mediated activation of Raf. *EMBO J.* **16,** 7019–7031 (1997).
36. Morse, H. C. III *et al.* Bethesda proposals for classification of lymphoid neoplasms in mice. *Blood* **100,** 246–258 (2002).
37. Donlon, J. A., Jaffe, E. S. & Braylan, R. C. Terminal deoxynucleotidyl transferase activity in malignant lymphomas. *N. Engl. J. Med.* **297,** 461–464 (1977).
38. Jaffe, E. S., Harris, N. L., Stein, H. & Vardiman, J. W. *Pathology and Genetics of Tumours of Haematopoietic and Lymphoid Tissues* (IARC Press, Lyon, France, 2001).
39. Whitehurst, C. E., Chattopadhyay, S. & Chen, J. Control of V(D)J recombinational accessibility of the D beta 1 gene segment at the TCR beta locus by a germline promoter. *Immunity* **10,** 313–322 (1999).
40. Gurrieri, C. *et al.* Loss of the tumor suppressor PML in human cancers of multiple histologic origins. *J. Natl Cancer Inst.* **96,** 269–279 (2004).
41. Alizadeh, A. A. *et al.* Distinct types of diffuse large B-cell lymphoma identified by gene expression profiling. *Nature* **403,** 503–511 (2000).
42. Rosenwald, A. *et al.* The use of molecular profiling to predict survival after chemotherapy for diffuse large-B-cell lymphoma. *N. Engl. J. Med.* **346,** 1937–1947 (2002).
43. Hans, C. P. *et al.* Confirmation of the molecular classification of diffuse large B-cell lymphoma by immunohistochemistry using a tissue microarray. *Blood* **103,** 275–282 (2004).
44. Shvarts, A. *et al.* A senescence rescue screen identifies BCL6 as an inhibitor of anti-proliferative $p19^{ARF}$-p53 signaling. *Genes Dev.* **16,** 681–686 (2002).
45. Lossos, I. S. *et al.* Prediction of survival in diffuse large-B-cell lymphoma based on the expression of six genes. *N. Engl. J. Med.* **350,** 1828–1837 (2004).
46. Sanchez-Beato, M., Sanchez-Aguilera, A. & Piris, M. A. Cell cycle deregulation in B-cell lymphomas. *Blood* **101,** 1220–1235 (2003).
47. Phan, R. T. & Dalla-Favera, R. The *BCL6* proto-oncogene suppresses p53 expression in germinal-center B cells. *Nature* **432,** 635–639 (2004).
48. Carnero, A., Hudson, J. D., Price, C. M. & Beach, D. H. p16INK4A and p19ARF act in overlapping pathways in cellular immortalization. *Nature Cell Biol.* **2,** 148–155 (2000).
49. Hedvat, C. V. *et al.* Application of tissue microarray technology to the study of non-Hodgkin's and Hodgkin's lymphoma. *Hum. Pathol.* **33,** 968–974 (2002).

Supplementary Information accompanies the paper on **www.nature.com/nature**.

Acknowledgements We thank D. Yao, C. Hedvat, M. Dudas, J. Qin and A. Wilton for assistance on TMA preparation, staining and statistical analyses; S. Hasan for assistance with data input and management; K. Manova, C. Farrell and other Molecular Cytology Core Facility members for advice and assistance with IHC; J. Overholser and other Monoclonal Antibody Core Facility staff for help with antibody generation; G. Cattoretti and R. Dalla-Favera for advice; and L. Khandker, L. Dong, M. Hu, L. DiSantis and other P.P.P. laboratory members for assistance and discussion. This work is supported in part by an NCI grant to P.P.P.

Competing interests statement The authors declare that they have no competing financial interests.

Correspondence and requests for materials should be addressed to P.P.P. (p-pandolfi@ski.mskcc.org).